Theoretical Investigation of Gas-Phase Thermal Reactions between Carbon Monoxide and Water

Shao-Wen Hu,*,† Shan-Mou Lü,‡ and Xiang-Yun Wang†

Department of Applied Chemistry, College of Chemistry and Molecular Engineering, Peking University, Beijing, China 100871, and Group of Physics, Affiliated High School of Peking University, Beijing, China 100871

Received: June 10, 2004; In Final Form: August 4, 2004

Ground-state potential energy surface of the CO−H_2O system was explored using ab initio calculations at the CCSD(T)/6-311++G**//MP2/6-311++G** level. Providing energy of about 74 kcal/mol, the initial bimolecular complex CO−H_2O can associate into formic acid (HCOOH) or dihydroxycarbene (HOCOH). Both HCOOH and HOCOH can further dissociate into CO_2 and H_2 through three reaction channels. Providing energy more than 100 kcal/mol, CO−H_2O complexes can dissociate into hydroxyl (OH) and formyl (HCO) radicals. Further association of the two radicals leads to formaldehyde carbonyl oxide, dioxirane, and some highly unstable species, including triangular CO_2 and linear carbon peroxide COO.

I. Introduction

Gas-phase reactions between carbon monoxide (CO) and water (H_2O) are of fundamental importance because the two molecules exist ubiquitously not only in the atmosphere[1] but also in interstellar molecular clouds.[2,3] Fundamental reactions of CO and H_2O, bridging small inorganic molecules to complicated organic functional groups, are indicative in elucidating the origin of life.[4−7] Industrially, the reaction CO + H_2O = H_2 + CO_2 turns H_2O into H_2, and this so-called water−gas shift has long been investigated for efficient fuel energy production.[8−10] In the atmosphere, some reactive molecules, such as formaldehyde carbonyl oxide (H_2COO), dioxirane (OCH_2O), and radicals HCO + OH, are found to be responsible for air pollution.[11−13] Because these species are all stoichemically the same as CO + H_2O, it is desirable to know whether and how they can convert to each other and to the more stable forms.[14−18]

The reactions, especially those involving stable molecules, have been studied extensively. It is in general accepted that two thermal reactions occur at ground state, CO + H_2O = HCOOH and HCOOH = H_2 + CO_2. Substantial activation energies are required for both reactions. The question is, on thermal decomposition of HCOOH, high-level theoretical calculations give quite close energy barriers for the two reaction channels, dehydration and decarboxylation of HCOOH, implying near equal amount of products, CO and CO_2, and unimolecular processes.[19−23] Some experimental observations, however, showed that the product ratio CO/CO_2 is as large as 10 and highly temperature dependent.[24,25] To explain the inconsistency between theory and experiments, the dissociated H_2O molecule is proposed as a catalyst.[22] Practically, to catalyze the water−gas shift reaction, two kinds of catalysts have to be used at low and high temperatures,[26,27] implying the coexistence of multiple reaction channels. In recent years, photochemical decomposition of HCOOH via electronic excited states has been studied.[28] As for thermal decomposition, likely to happen at the ground state, a more complete investigation is still necessary.

In this work, the CO + H_2O system is reexamined theoretically. To avoid more complications, only the singlet ground-state potential energy surface (SGPES) was explored. Compared to previouly published works by others, we investigate the system in a wider energy range and included more possible intermediate species. Our intention is to give a more complete picture of all possible reaction channels so as to interpret or predict the relevant experimental results.

II. Calculation Method

The geometry structures were fully optimized at the MP2 = Full/6-31+G* and MP2 = Full/6-311++G**level. Transition states were located using synchronous transit-guided quasi-Newton (STQN) methods[29] in combination with stepwise partial optimization along each pathway with one geometric parameter fixed as constant. Frequency calculations were performed by following each optimization to obtain the zero point energy (ZPE) and to characterize all the stationary points located on the potential energy surface. Intrinsic reaction coordinate (IRC) calculations were performed to confirm the relationship of each transition state with its reactant and product. Single point calculations at the CCSD(T) = Full/6-311++G**levels were performed to determine the electronic energies. The relative energies reported in our discussion and showed in figures of pathways are obtained at the CCSD(T) = Full/6-311++G** level with MP2 = Full/6-311++G** calculated ZPE corrections. The Guassian 98 program package[30] was employed for these calculations.

III. Results and Discussions

To evaluate the accuracy of the calculated energies, results of a few species obtained at different level of theories are listed in Table 1. Energies calculated at three different theoretical levels are listed together with dipole moments and rotational constants for all the species in Table 2 of the Supporting Information. It can be seen that using a larger basis set

* Corresponding author. E-mail: sw-hu@163.com.
† Peking University.
‡ Affiliated High School of Peking University.

10.1021/jp047486g CCC: $27.50
Published on Web 09/09/2004

TABLE 1: Comparison of Relative Energies of a Few Species Using Different Methods[a]

	8	TS **4**	**12**	**16**	**17**	TS **19**
MP2/6-31+G*//MP2/6-31+G*[b]	0.00	73.64	83.55	5.43	80.84	14.22
MP2/6-311++G**//MP2/6-311++G**[b]	0.00	70.53	80.01	4.64	84.64	13.20
CCSD(T)/6-311++G**//MP2/6-311++G**[b]	0.00	72.41	80.03	4.53	87.23	12.68
TZ+2PCCSDT-1//DZ+PCCSDT-1[c]	0.00	73.71	83.77	4.47	80.42	13.37

[a] Electronic energies (kcal/mol) without correction of ZPE. [b] Values calculated in this work. [c] Values taken from ref 19.

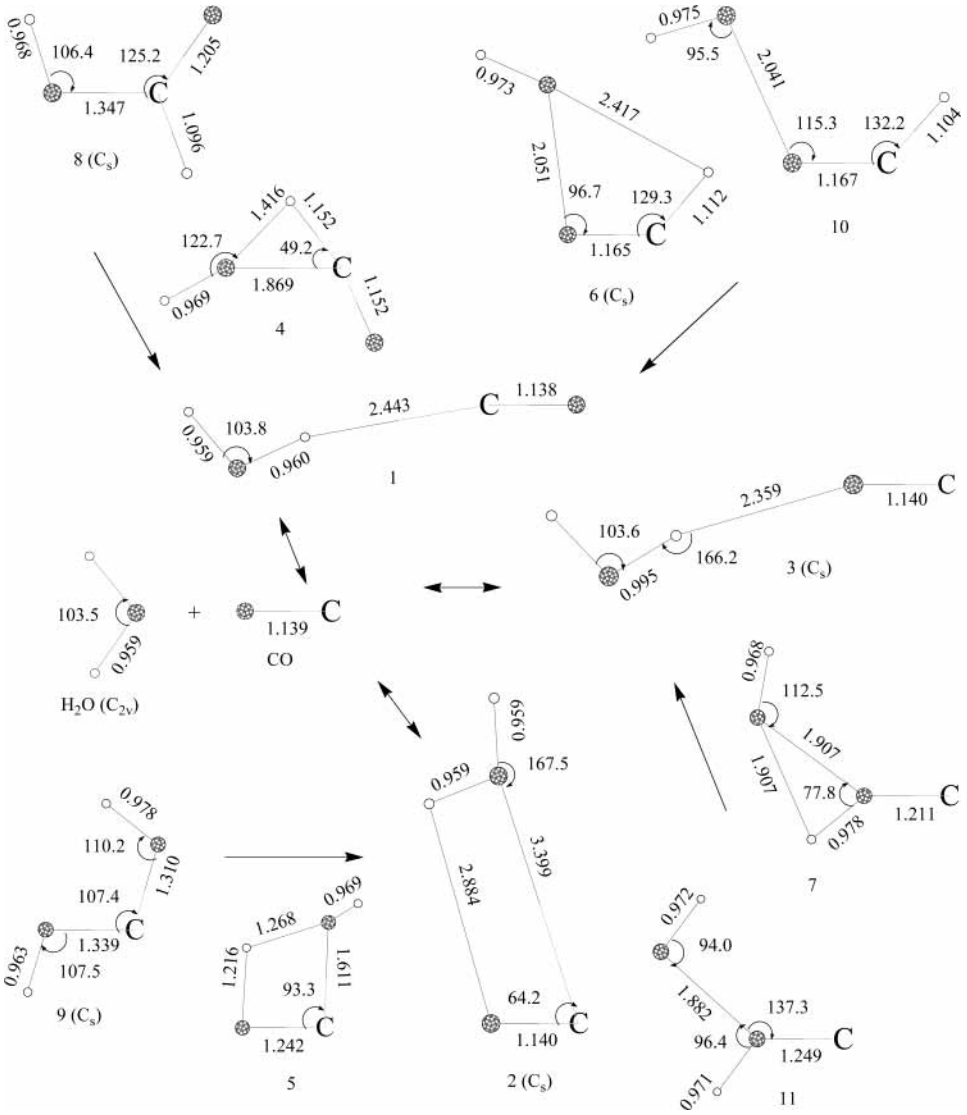

Figure 1. Species involved in the initial steps of reactions between CO and H_2O; bond lengths are in Å; angles are in degrees; the species beside arrows are transition states; the direction of arrows is toward energy descent; in parentheses, the symmetry of the species is indicated, except for C_1.

(6-311++G** instead of 6-31+G*) lowers the electronic energies significantly, whereas using a method including more effective electron correlation (CCSD instead of MP2) has a less impact. Generally, relative energies calculated at the MP2/6-311++G** level are quite close to those calculated at the CCSD(T)/6-311++G** level and consistent with the results reported in the literature.[19] Therefore, we believe that the probable errors of our final reported relative energies for the various species are less than 5 kcal/mol.

Vibrational frequencies calculated at the MP2/6-311++G** level are listed in Table 3 of the Supporting Information for all intermediate species.

Each stationary point on the SGPES was given a number. The letters "TS" were added to specify the transition state.

Geometry structures (MP2 = Full/6-311++G** calculation) of the species were shown as reactants, transition states, intermediates, or products (Figures 1, 3, 5, 7, 9, 11). Reaction pathways with relative energies of the species are summarized in a single figure (Figure 2) as well as in separate figures (Figures 4, 6, 8, 10, 12).

The reactions between CO and H_2O were assumed to start from their weakly bonded complex, CO−H_2O. Three such complexes were located, **1**, **2**, and **3**. Two kinds of hydrogen bonds, H−C and H−O, are responsible for the formation of **1** and **3**. As hydrogen-bond acceptor, oxygen seems slightly stronger than carbon, because H−O in **2** is slightly shorter than H−C in **1**. These two bimolecular complexes have been studied in detail previously.[31−35] We located another complex **2** on the

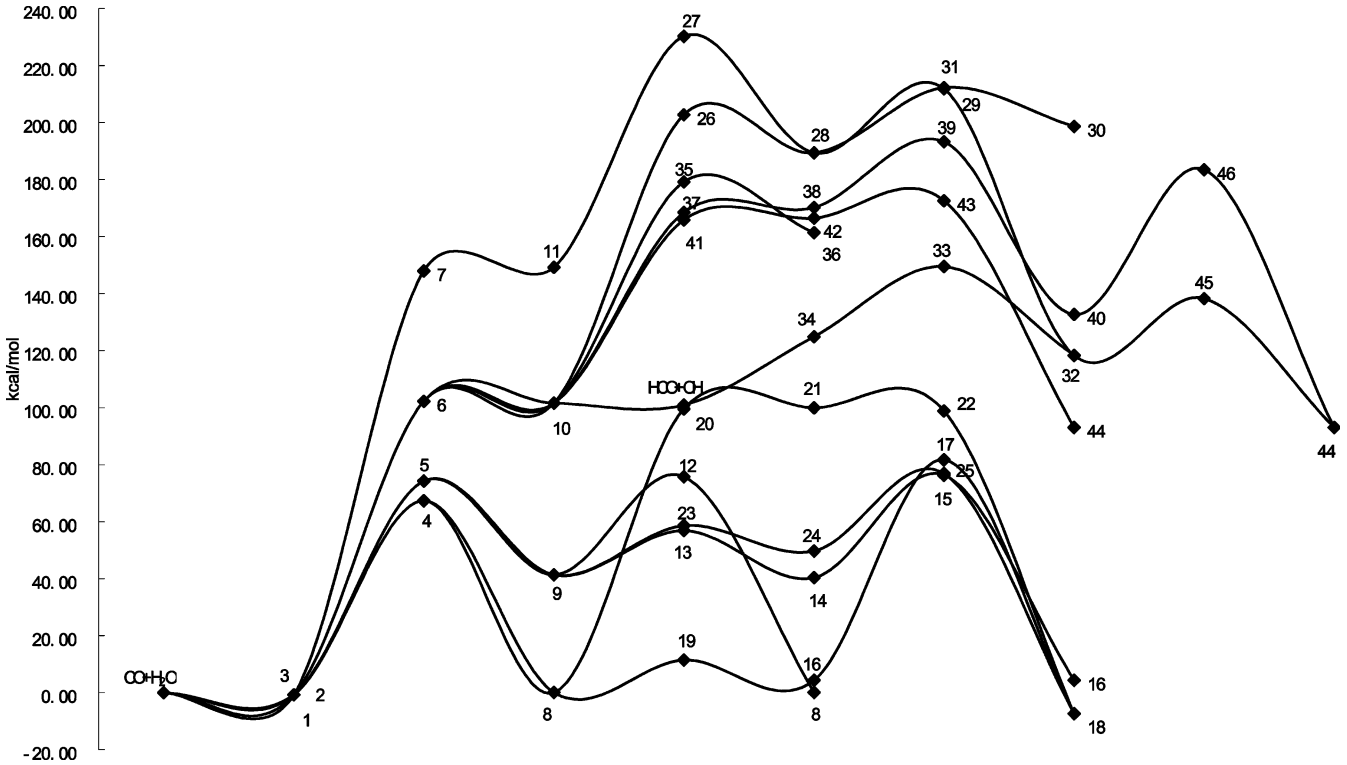

Figure 2. Total reaction pathways on the SGPES of the CO−H_2O system. See Figure 1, 3, 5, 7, 9, and 11 for geometry structures of the numbered species. Relative energies are values calculated at the CCSD(T)/6-311++G**//MP2/6-311++G** level with ZPE correction.

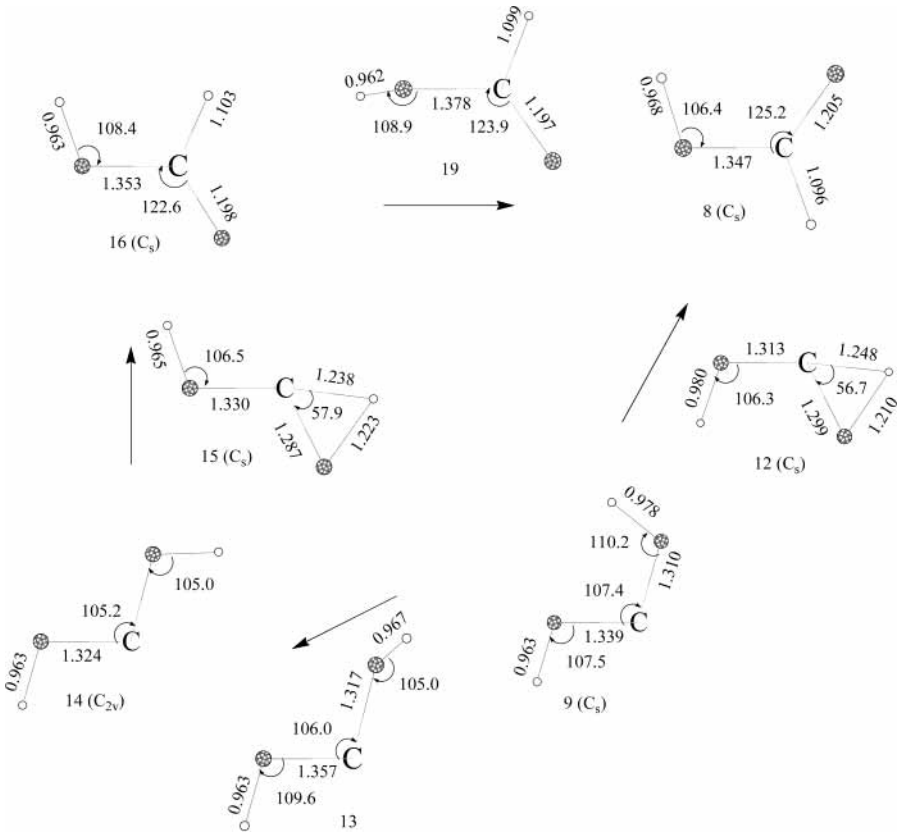

Figure 3. Species involved in pathways from HOCOH (**9**) to HCOOH (**8**); bond lengths are in Å; angles are in degrees; the species beside arrows are transition states; the direction of arrows is toward energy descent; in parentheses, the symmetry of the species is indicated, except for C_1.

SGPES. This loose four-member ring structure, however, may not be a true minimum using other levels of theoretical methods. Nevertheless, the SGPES is rather flat at this part and the binding energies of all the bimolecular complexes are all less than 1 kcal/mol. Assigning the energy sum of CO and H_2O as 0.00 kcal/mol, the relative energies of **1**, **2**, and **3** are −0.74, −0.69, and −0.75 kcal/mol, respectively. Because energetically indistinguishable, the CO−H_2O complexes as well as their separated

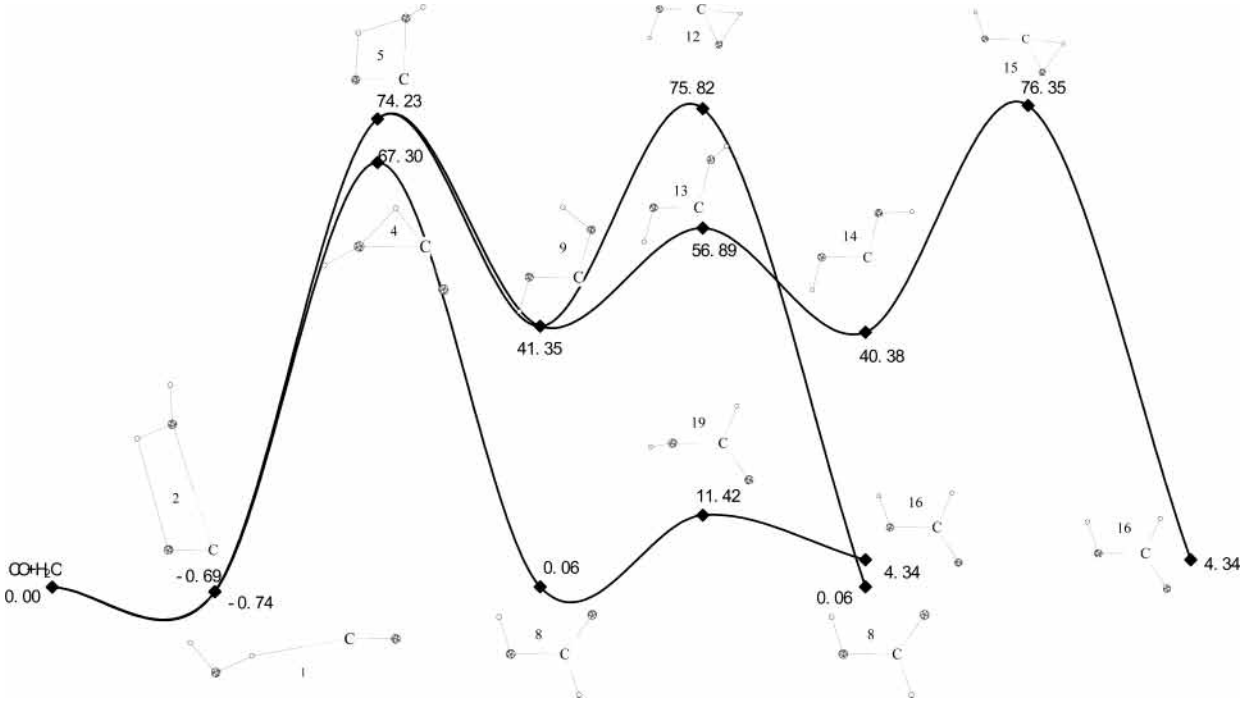

Figure 4. Reaction pathways connecting CO and H_2O to HCOOH on the SGPES of the CO−H_2O system. See Figures 1 and 3 for detailed geometry structures of the numbered species. Relative energies (in kcal/mol) are values calculated at the CCSD(T)/6-311++G**//MP2/6-311++G** level with ZPE correction.

form are equally distributed conformers at the inactivated initial stage. Their different molecular orientations indicate the potential of further reactions.

To initiate the reaction between CO and H_2O, at least 68.04 kcal/mol energy is required. With this lowest energy, the system can be activated to a transition state (TS), **4**, from **1**. In the process, the original hydrogen bond O−H−C shortens and an O−C bond forms. As the three-membered ring in **4** breaks at the hydrogen bridge, formic acid HCOOH (**8**) forms with an energy fall to 0.80 kcal/mol relative to **1**. In previous works, the transition state **4** has been located on the pathway of dehydration of formic acid.[21,22] The reverse reaction happens via the same path with **1** as precursor for easiest HCOOH formation. Starting from **2**, over an energy barrier of 74.92 kcal/mol, the system can be activated to TS **5**. In the four-membered ring structure of **5**, hydrogen bridges two oxygen atoms from H_2O and CO and an O−C bond forms simultaneously. As a result, the direct product is a conformer of dihydroxycarbene HOCOH (**9**) rather than formic acid. The energy of **9** is 41.29 kcal/mol relative to **8**. It is worthwhile to note that the second barrier is only 6.88 kcal/mol higher than the first one, indicating that the two kinds of reactions are competitive.

Raising the system's energy to higher level, dissociation via radical pathways becomes probable. Starting from **1**, the system can be activated to TS **6** with 102.93 kcal/mol energy and produce HCO−OH (**10**), a singlet biradical structurally and energetically similar to **6**. In **6** and **10**, H_2O donates one of its H to the C of CO, leaving the hydroxyl radical OH loosely bonded to formyl radical HCO. Alternatively, starting from **3**, the system can be activated to TS **7** with 148.69 kcal/mol energy and produce COH−OH (**11**), another singlet biradical structurally and energetically close to **7**. In **7** and **11**, H_2O donates one of its H to the O of CO, leaving the OH group loosely bonded to COH radical.

These are four probable reactions that are able to happen depending on different initiating energies. Over subsequent energy barriers, the reaction path starting from the four initial products can lead to other intermediates and products. The total reaction pathways, shown in Figure 2, were divided into four parts for clarity and convenience in the following discussion.

Part I: Pathways from CO + H_2O to HCOOH. Beside the path with lowest energy of 68.04 kcal/mol via TS **4**, two indirect paths via formation of intermediate dihydroxycarbene **9** lead the CO−H_2O bimolecular complexes to HCOOH. Starting from **9**, four competitive reaction channels exist. The first channel leads back to CO−H_2O via TS **5**. The energy barrier is 32.89 kcal/mol. The second channel leads to HCOOH via 1,2-hydrogen transfer, as shown by TS **12**. The energy barrier is 34.36 kcal/mol. The third channel consists of two steps, isomerizing from **9** to HOCOH (**14**), a slightly more stable conformer of dihydroxycarbene, followed by another 1,2-hydrogen transfer, as shown by TS **13** and TS **15**, resulting in *cis*-HCOOH (**16**). The energy barrier is 15.55 kcal/mol for the first step and 35.97 kcal/mol for the second step. The barrier of cis−trans HCOOH isomerization, as shown by TS **19**, is only 7.07 kcal/mol and is hardly to be considered as one of the steps. The fourth channel, which also consists of two steps, results in CO_2 and H_2 rather than HCOOH and will be discussed in part II. Therefore, if the energy of the system reaches to 76.35 kcal/mol relative to the initial stage, the gas-phase reaction between CO and H_2O can produce HCOOH via three channels, a single-step process, a two-step process involving dihydroxycarbene as intermediate, and a three-step process involving dihydroxycarbene and its conformational change. The geometry structures of the species involved in this part are shown in Figures 1 and 3. The reaction pathways are shown in Figure 4.

Part II: Pathways from CO + H_2O to CO_2 + H_2. From CO + H_2O to CO_2 + H_2, no single-step routes are found. The final products can be produced via three channels. Two of them have to form HCOOH as an intermediate. With an activation energy of 77.37 kcal/mol, the two H atoms in *cis*-HCOOH (**16**)-can associate into an H_2 molecule and then eliminate, leaving the linear CO_2, as shown by TS **17**. The product H_2−CO_2 (**18**) is a weakly bonded complex of H_2 and CO_2. Its energy is −6.65

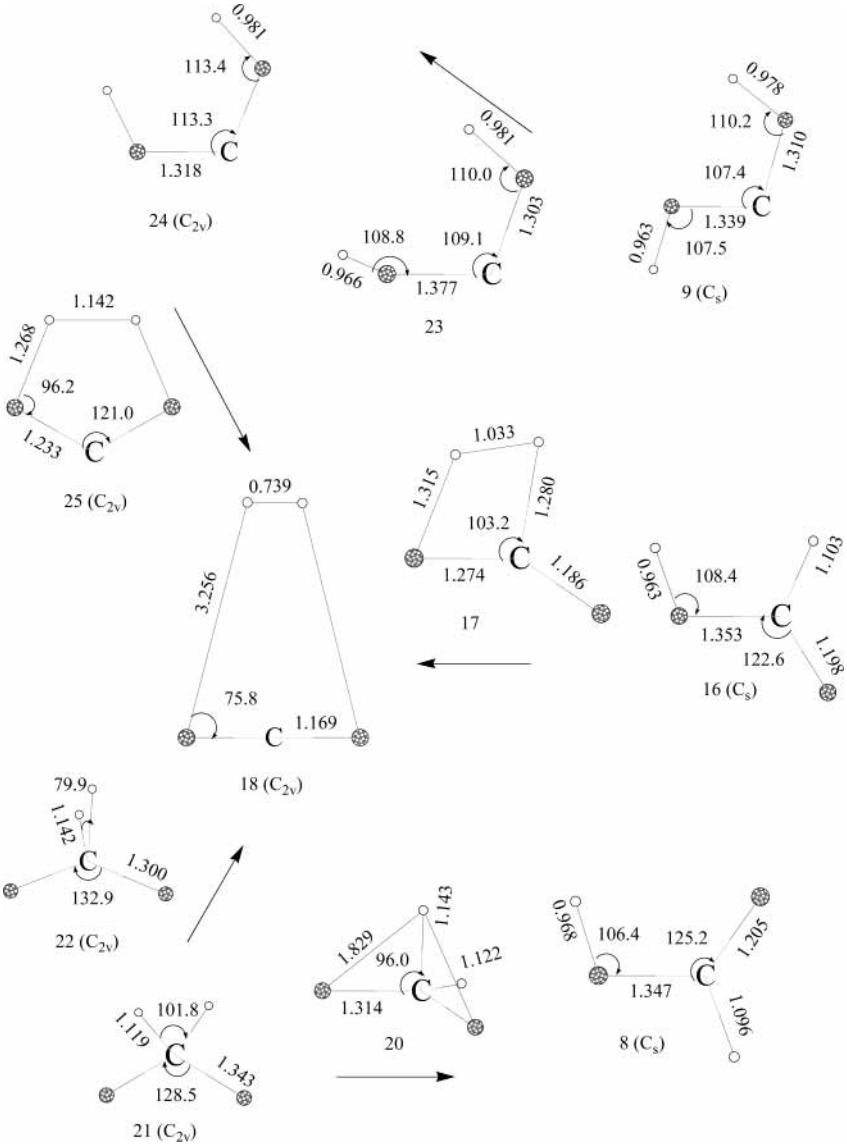

Figure 5. Species involved in three reaction pathways lead to $CO_2 + H_2$; bond lengths are in Å; angles are in degrees; the species beside arrows are transition states; the direction of arrows is toward energy descent; in parentheses, the symmetry of the species is indicated, except for C_1.

kcal/mol relative to **1**. With an activation energy of 99.58 kcal/mol, the H atom of the OH group in HCOOH can transfer to carbon, as shown by TS **20**. The direct product is dioxymethane OCH_2O (**21**) with C_{2v} symmetry. The energy of **21** is almost the same as those of TS **20** and the following transition state **22**, indicating its transient nature. As shown by **22**, when the two H associate into H_2 and then eliminates, the O−C−O angle becomes larger and CO_2 forms. Because the energy of TS **20** is 22.21 kcal/mol higher than that of TS **17**, the chance of decarboxylation via the second channel is significantly less probable than the first one. As mentioned in part I, started from **9**, there is a channel that leads to CO_2. This is a two-step process. First, over a barrier of 17.24 kcal/mol, another conformer of dihydroxycarbene $C(OH)_2$ (**24**) can form from **9**. The transition state for the conformational change is **23**. The cis position of the two H atoms in **24** is potentially possible to associate into H_2 and eliminate, as shown by TS **25**, resulting in **18**. The barrier height for the H_2 elimination is 76.84 kcal/mol. Therefore, it may be important to note that the stable formic acid does not have to be the only intermediate connecting initial and final bimolecular complexes, CO−H_2O and H_2−CO_2 (**18**); the water−gas shift reaction can also be mediated by dihydroxycarbene. Examining the structures of **2**, **9**, **24**, and **18**, it can be seen that if H_2O is forced to approach CO in the vertical direction as in **2**, the reaction along this path may be favored.

Taking the results of part I into consideration, the discrepancy in terms of HCOOH decomposition can be interpreted as following. Dehydration of HCOOH has three reaction channels with energy barriers below 76.35 kcal/mol, whereas decarboxylation of HCOOH has two reaction channels with energy barriers of 5.37 and 23.29 kcal/mol higher. Therefore, the ratio of CO/CO_2 is large and highly temperature dependent.

The reverse of the reaction pathways is hydrogenation of CO_2. Initially, H_2 and CO_2 associate loosely, as in **18**. It can be seen that hydrogenation takes place not only with quite high energy barriers but also results in two kinds of competitive products, CO + H_2O and HCOOH. Therefore, catalysts are found to play an important role in the process.[36]

Part III: Pathways from Dioxirane to CO + H_2O. As we have mentioned above, at relative high temperatures, the CO−H_2O system can dissociate into hydroxyl and formyl radicals. The two radicals OH and HCO can associate via an O−O bond into formyl hydroxide HCO−OH (**34**). The association is an energy-increasing process. The energy of **34** is 23.93 kcal/mol relative to the energy sum of OH and HCO. With 24.64 kcal/mol more energy, the hydroxyl hydrogen in **34** can transfer to

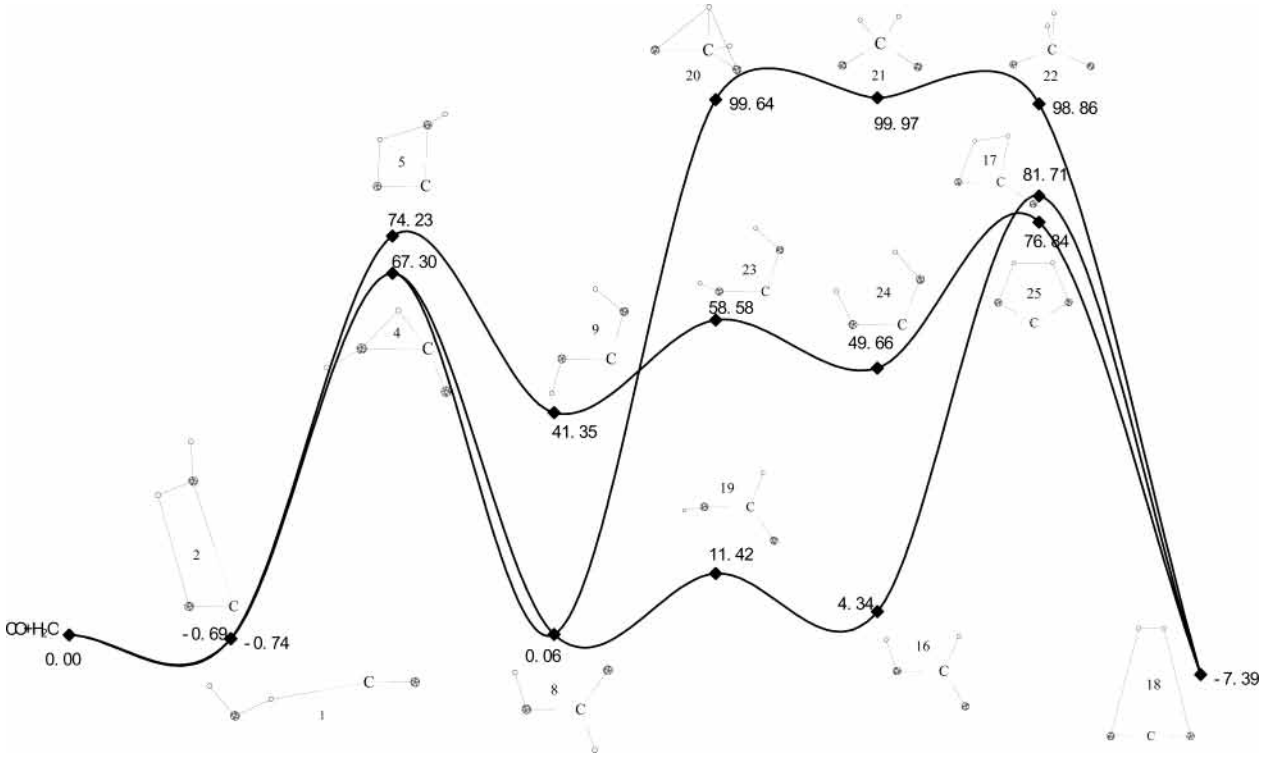

Figure 6. Reaction pathways connecting CO and H_2O to CO_2 and H_2 on the SGPES of the CO−H_2O system. See Figures 1, 3, and 5 for detailed structures of the numbered species. Relative energies (in kcal/mol) are values calculated at the CCSD(T)/6-311++G**//MP2/6-311++G** level with ZPE correction.

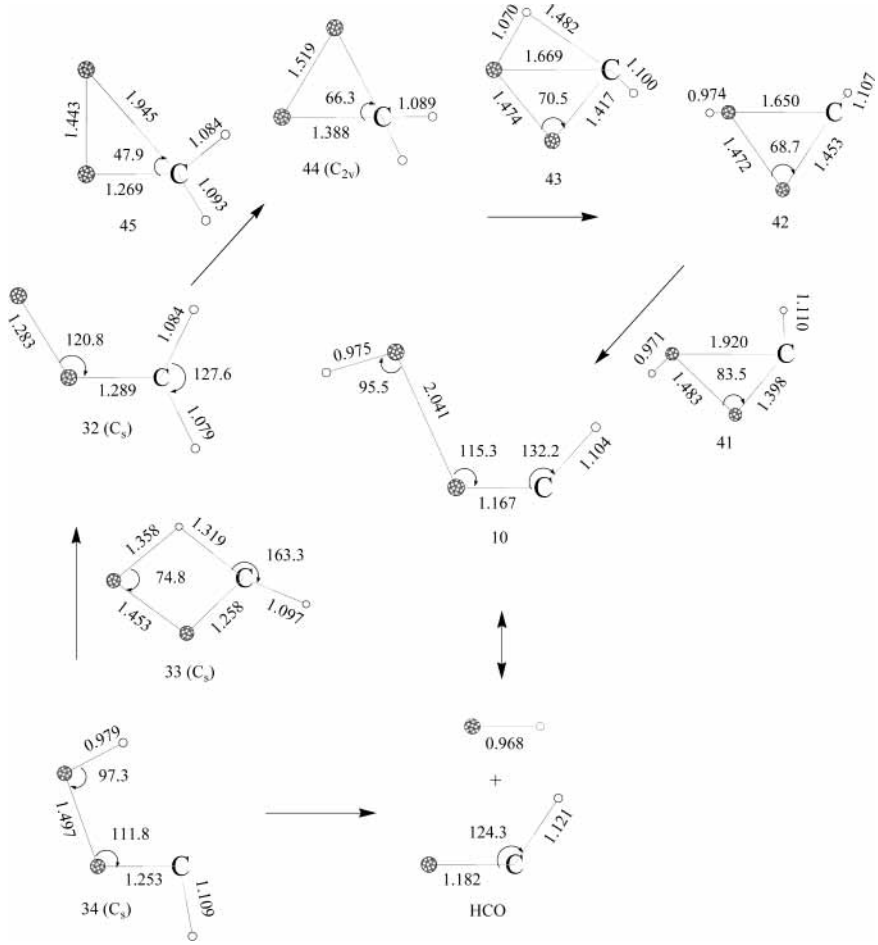

Figure 7. Species involved in reaction pathways from HCO−OH (**10**) to dioxirane (**44**); bond lengths are in Å; angles are in degrees; the species beside arrows are transition states; the direction of arrows is toward energy descent; in parentheses, the symmetry of the species is indicated, except for C_1.

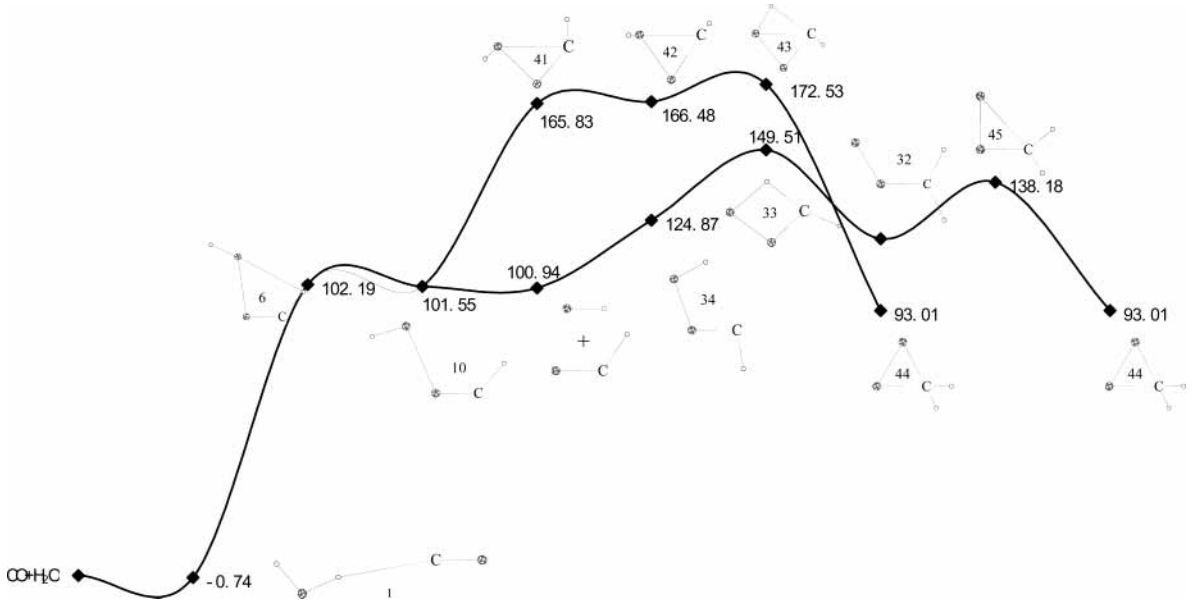

Figure 8. Reaction pathways connecting CO and H_2O to dioxirane **44** on the SGPES of the CO−H_2O system. See Figures 1 and 7 for detailed structures of the numbered species. Relative energies (in kcal/mol) are values calculated at the CCSD(T)/6-311++G**//MP2/6-311++G** level with ZPE correction.

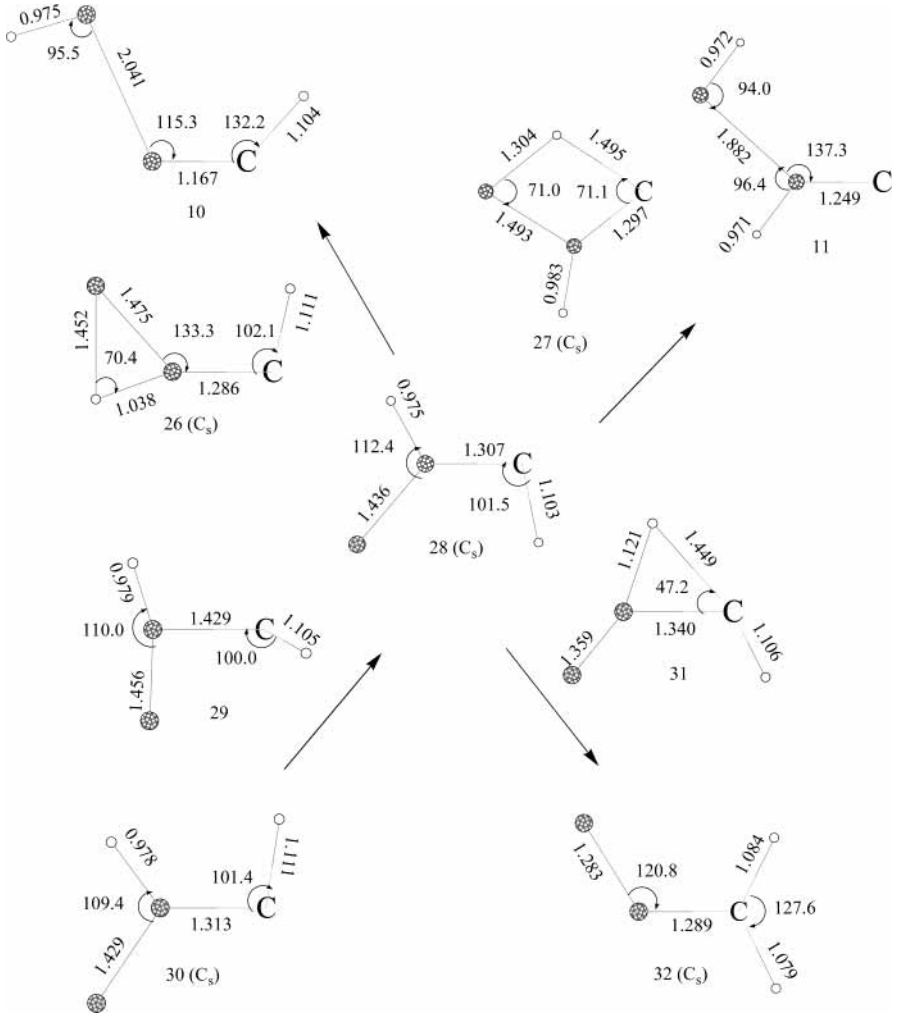

Figure 9. Species involved in reaction pathways from HCO−OH (**10**) to OOHCH (**28**) and CH_2OO (**32**); bond lengths are in Å; angles are in degrees; the species beside arrows are transition states; the direction of arrows is toward energy descent; in parentheses, the symmetry of the species is indicated, except for C_1.

carbon as shown by TS **33**, resulting in formaldehyde carbonyl oxide H_2COO (**32**). The energy of **32** is 6.53 kcal/mol lower than that of **34**, but still 17.40 kcal/mol higher than that of OH + HCO, due to the reactive O−O bond. Over a barrier of 19.85

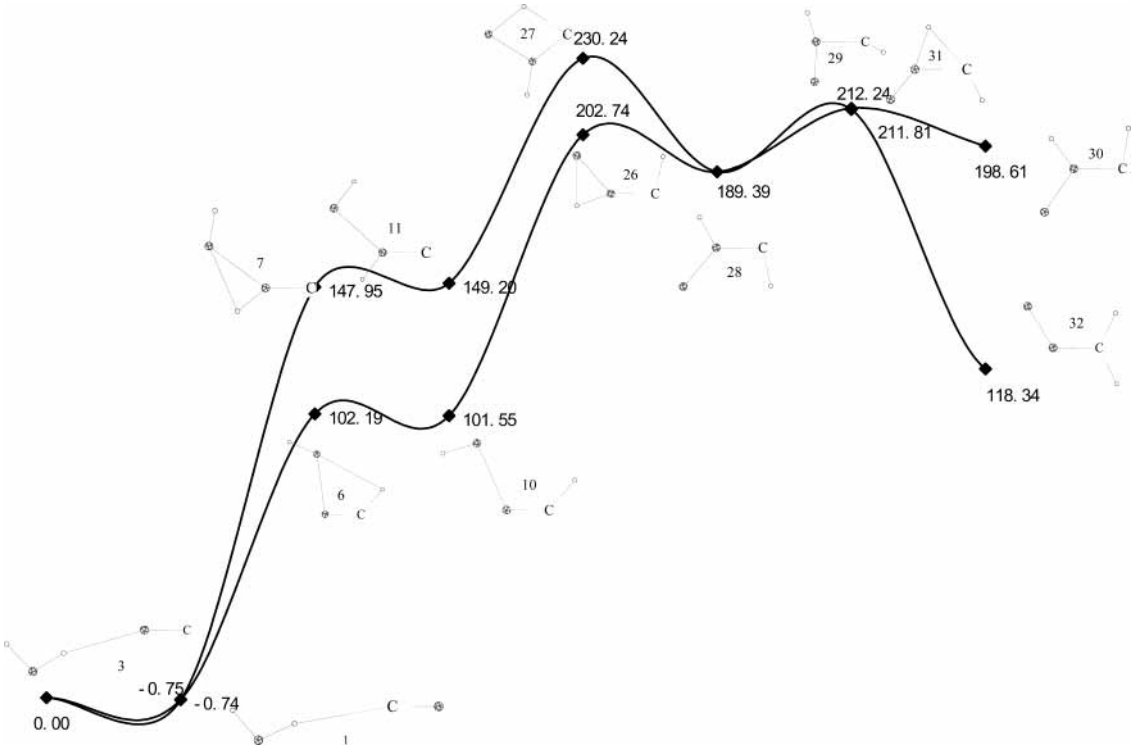

Figure 10. Reaction pathways connecting CO and H_2O to CH_2OO via OOHCH (**28**) on the SGPES of the CO−H_2O system. See Figures 1 and 9 for detailed structures of the numbered species. Relative energies (in kcal/mol) are values calculated at the CCSD(T)/6-311++G**//MP2/6-311++G** level with ZPE correction.

kcal/mol, formaldehyde carbonyl oxide **32** can convert to dioxirane CH_2O_2 (**44**) with an energy fall of 25.33 kcal/mol. The ring closing transition state is **45**. In previous work, part of the reaction pathway starting from **44** to OH + HCO was revealed.[14] Our contribution here is relating **44** to CO and H_2O. According to our calculations, OH and HCO can associate into biradical **10** and then go to CO and H_2O without barrier. In environmental measurements, the concentrations of CO and OH are found to be correlated.[37−39] On biological observation, the poisoning effect of CO to animals also has some relations with OH.[40,41] It is thus important to reveal the reaction channels connecting the two species.

Providing 64.28 kcal/mol energy to **10**, a bond between hydroxyl oxygen and carbon can form, as shown by TS **41**. This process results in a high-energy intermediate, *trans*-HOCOH (**42**) with a three-membered ring structure. Over a small barrier of 6.05 kcal/mol, hydrogen migrates from oxygen to carbon, as shown by TS **43**, resulting in dioxirane **44**. Reaction along this route is more energy demanding. Therefore, dioxirane is likely to convert to formaldehyde carbonyl oxide **32**, CO, and H_2O with **45** as an intermediate.

It was reported that dioxirane can convert to CO_2 via a ring-opening process, and a O−O bond half breaking transition state has been located.[16] However, we cannot locate such a transition state on the SGPES. It seems to us neither a technical problem nor due to calculation methods. Instead, we guess that the ring-opening process is more likely to happen via electronic excited singlet or triplet states.

Part IV: Pathways from Hydroperoxylcarbene OOHCH (28) to CO + H_2O. Hydroperoxylcarbene OOHCH (**28**) is another transient species located as intermediate between biradical species **10**, **11**, and formaldehyde carbonyl oxide **32**. Starting from **28**, only 13.36 kcal/mol is required for the −OH− hydrogen transfer to the terminal oxygen, as shown by TS **26**, resulting in **10**. Accompany the formation of OH−HCO biradical and CO + H_2O, the system's energy falls substantially. Over a barrier of 22.42 kcal/mol, the hydroxyl hydrogen in **28** can transfer from oxygen to carbon, as shown by TS **31**, resulting in formaldehyde carbonyl oxide **32**. It is more energy demanding for hydrogen to transfer from carbon to the terminal oxygen, resulting in biradical **11** and then CO + H_2O. The barrier is 40.85 kcal/mol and the transition state is **27**. There are no reports about the existence of **28**. On the SGPES of the system, no species with the same elemental composition are found to be in higher energy, except for **30**, in which the two hydrogen atoms are in cis position to each other. The cis conformer of **28** is OOHCH (**30**), with an energy of 9.23 kcal/mol higher than that of **28**, and only 13.63 kcal/mol energy is required for the conformational change from **30** to **28**. The transition state is **29**. The tentative nature of **28** or **30** may result from the three-coordinated oxygen.

Part V: Pathways from OCO + H_2 and COO + H_2 to CO + H_2O. It can be seen from part III that the species connecting to biradical **10** or **11** in the reaction pathways all contain a reactive O−O bond. Two more such species were located as minimum on the high-energy part of the SGPES. Providing 66.91 kcal/mol energy to **10**, hydroxyl oxygen can bond to carbon to form a three-membered ring structure as shown by transition state **37** and intermediate *cis*-HOCOH (**38**). Over a subsequent barrier of 24.84 kcal/mol, the two hydrogen atoms, with cis position to each other, can associate into a hydrogen molecule and eliminate as shown by TS **39**, leaving a three-membered ring structure of carbon dioxide loosely bonded to H_2 in $OCOH_2$ (**40**). The eliminated hydrogen molecule can associate to the carbon of the triangular CO_2 as shown by TS **46**, resulting in dioxirane **44**. The energy barrier for the process is 50.75 kcal/mol relative to **40**. Providing 77.62 kcal/mol energy to **10**, hydroxyl hydrogen can associate with

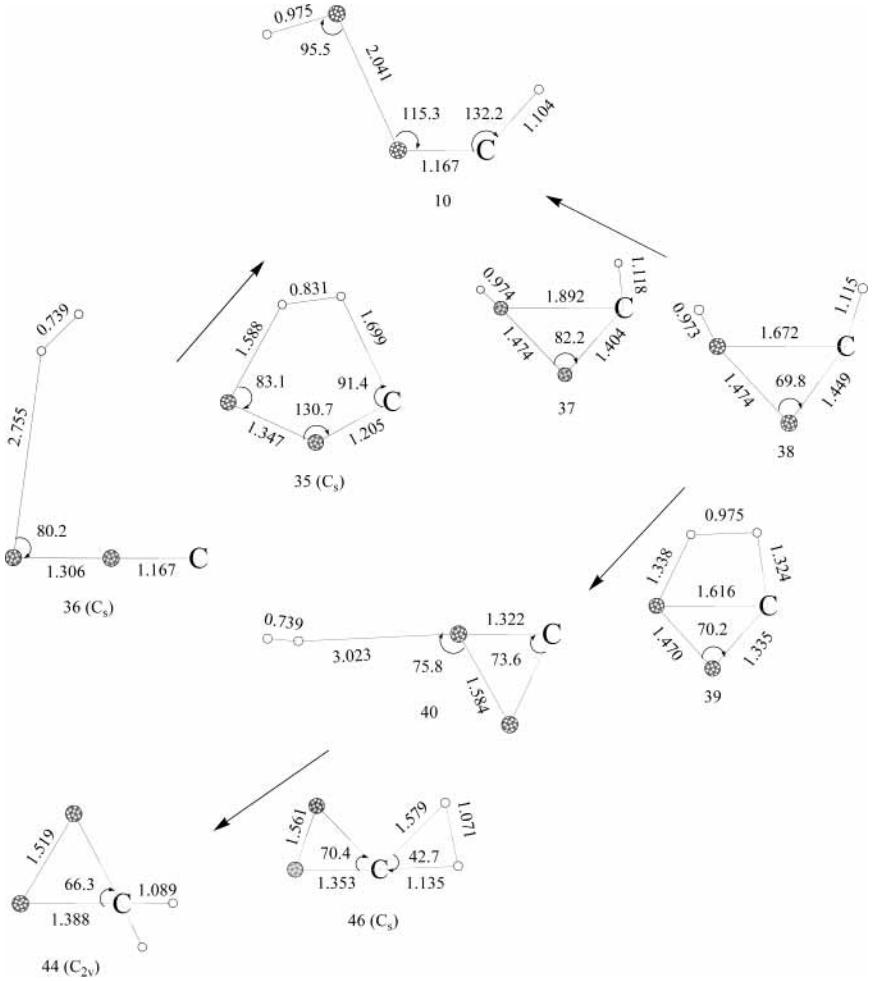

Figure 11. Species involved in reaction pathways from HCO−OH (**10**) to COO, OCO, and OCH_2O; bond lengths are in Å; angles are in degrees; the species beside arrows are transition states; the direction of arrows is toward energy descent; in parentheses, the symmetry of the species is indicated, except for C_1.

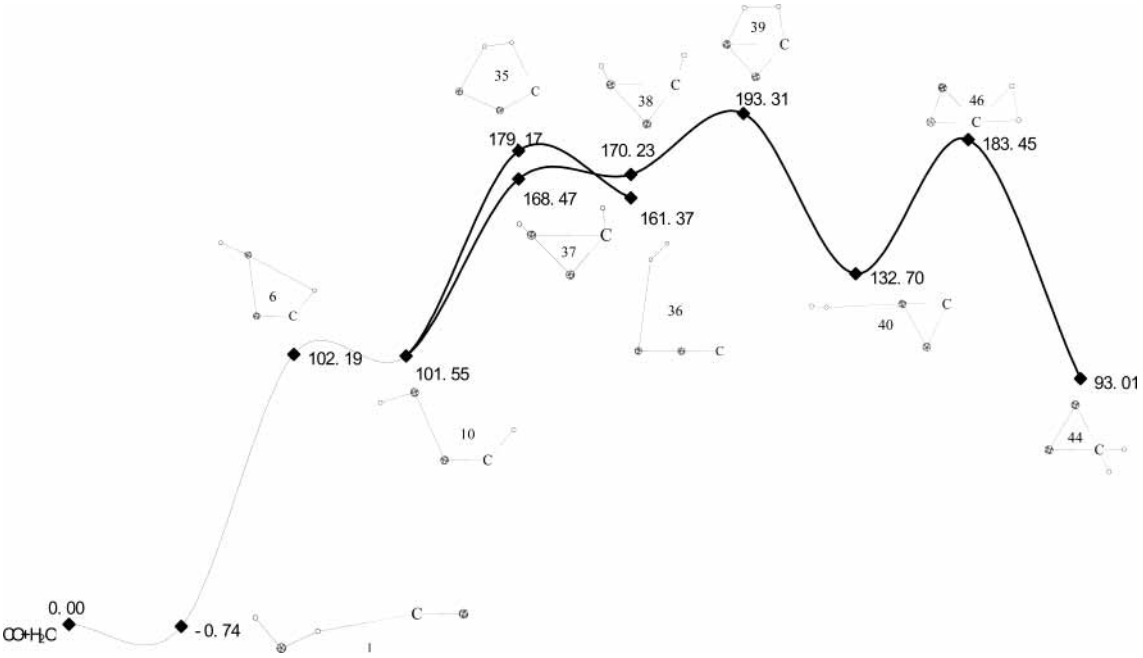

Figure 12. Reaction pathways connecting CO and H_2O to triangular CO_2 (**40**) and COO (**36**) on the SGPES of the CO−H_2O system. See Figures 1 and 11 for detailed structures of the numbered species. Relative energies (in kcal/mol) are calculated at the CCSD(T)/6-311++G**//MP2/6-311++G** level with ZPE correction.

carbon hydrogen directly into H_2 and then eliminate, as shown by TS **35**, leaving $COOH_2$ (**36**), a loosely bonded complex of H_2 and carbon peroxide COO. Bent carbon dioxide has been detected in crystal form.[42] There are still no reports on the

existence of COO in any form, although it seems to be a transient species resulting from direct association between atomic carbon and molecular oxygen.

IV. Concluding Remarks

In the gas phase, CO and H_2O form loosely bonded bimolecular complexes. Started from these complexes, thermal reactions can take place via different channels, depending on the temperature of the system. With activation energy up to 74.23 kcal/mol, two competitive reaction channels lead CO and H_2O to HCOOH and dihydroxycarbene, respectively. The unstable intermediate dihydroxycarbene can convert to HCOOH or $CO_2 + H_2$. Starting from HCOOH, three reaction channels lead to dehydration product CO and H_2O, whereas two channels lead to decarboxylation products $CO_2 + H_2$ with substantially higher energy barrier. Providing activation energy up to 102.19 kcal/mol, hydrogen transfer from H_2O to CO results in OH and HCO biradical, from which formaldehyde carbonyl oxide and dioxirane can be produced. With activation energy up to 147.95 kcal/mol, hydrogen transfer from H_2O to CO can result in OH and COH biradical. Other species containing an O−O bond, lying in high-energy parts on the SGPES, all connect to CO and H_2O via radical pathways. In these high-energy parts, however, electrons can be excited to higher states. A more complete picture of reaction pathways should include such states.

Supporting Information Available: Tables listing the electronic energies, dipole moments, and rotational constants of the species and the calculated vibrational frequency and IR intensity of the intermediate species. This material is available free of charge via the Internet at http://pubs.acs.org.

References and Notes

(1) Holloway, T.; Levy, H.; Kasibhatla, P. *J. Geophys. Res-Atmos.* **2000**, *105*, 12123.
(2) DiSanti, M. A.; Mumma, M. J.; Dello, R. N.; Magee-Sauer, K.; Novak, R.; Rettig, T. W. *Nature* **1999**, *399*, 662.
(3) Biver, N.; Rauer, H.; Despois, D.; Moreno, R.; Paubert, G.; BockeleeMorvan, D.; Colom, P.; Crovisier, J.; Gerard, E.; Jorda, L. *Nature* **1996**, *380*, 137.
(4) Takano, Y.; Ohashi, A.; Kaneko, T.; Kobayashi, K. *Appl. Phys. Lett.* **2004**, *84*, 1410.
(5) Huber, C.; Eisenreich, W.; Hecht, S.; Wachtershausher, G. *Science* **2003**, *301*, 938.
(6) Miyakawa, S.; Yamanashi, H.; Kobayashi, K.; Cleaves, H. J.; Miller, S. L. *P. Natl. Acad. Sci. U.S.A.* **2002**, *99*, 14628.
(7) Ryter, S. W.; Otterbein, L. E. *Bioessays* **2004**, *26*, 270.
(8) Farrauto, R.; Hwang, S.; Shore, L.; Ruettinger, W.; Lampert, J.; Giroux, T.; Liu, Y.; Ilinich, O. *Annu. Rev. Mater. Res.* **2003**, *33*, 1.
(9) Song, C. S. *Catal. Today* **2002**, *77*, 17.
(10) Fu, Q.; Saltsburg, H.; Flytzani-Stephanopoulos, M. *Science* **2003**, *301*, 935.
(11) Reeves, C. E.; Penkett, S. A. *Chem. Rev.* **2003**, *103*, 5199.
(12) Donahue, N. M.; Kroll, J. H.; Anderson, J. G.; Demerjian, K. L. *Geophys. Res. Lett.* **1998**, *25*, 59.
(13) Paulson, S. E.; Sen, A. D.; Liu, P.; Fenske, J. D.; Fox, M. J. *Geophys. Res. Lett.* **1997**, *24*, 3193.
(14) Gutbrod, R.; Kraka, E.; Schindler, R. N.; Cremer, D. *J. Am. Chem. Soc.* **1997**, *119*, 7330.
(15) Richardson, N. A.; Rienstra-Kiracofe, J. C. Schaefer, H. F. *Inorg. Chem.* **1999**, *38*, 6271.
(16) Anglada, J. M.; Bofill, J. M.; Olivella, S.; Sole, A. *J. Phys. Chem. A* **1998**, *102*, 3398.
(17) Aplincourt, P.; Henon, E.; Bohr, F.; Ruiz-Lopez, M. F. *Chem. Phys.* **2002**, *285*, 221.
(18) Kim, S. J.; Schaefer, H. F. *J. Phys. Chem. A* **2000**, *104*, 7892.
(19) Goddard, J. D.; Yamaguchi, Y.; Schaefer, H. F. *J. Chem. Phys.* **1992**, *96*, 1158.
(20) Francisco, J. S. *J. Chem. Phys.* **1992**, *96*, 1167.
(21) Ruelle, P.; Kesselring, U. W.; Ho, N. *J. Am. Chem. Soc.* **1986**, *108*, 371.
(22) Ruelle, P. *J. Am. Chem. Soc.* **1987**, *109*, 1722.
(23) Yagasaki, T.; Saito, S.; Ohmine, I. *J. Chem. Phys.* **2002**, *117*, 7631.
(24) Blake, P. G.; Davies, H. H.; Jackson, G. E. *J. Chem. Soc. B* **1971**, 1923.
(25) Corkum, R,; Willis, C.; Back, R. A. *Chem. Phys.* **1977**, *24*, 13.
(26) Van der Laan, G. P.; Beenackers, A. A. C. M. *Catal. Rev.* **1999**, *41*, 255.
(27) Rhodes, C.; Hutchings, G. J.; Ward, A. M. *Catal. Today* **1995**, *23*, 43.
(28) He, H. Y.; Fang, W. H. *J. Am. Chem. Soc.* **2003**, *125*, 16139.
(29) Peng, C. Y.; Ayala, P. Y.; Schlegel, H. B.; Frisch, M. J. *J. Comput. Chem.* **1996**, *17*, 49.
(30) Frisch, M. J.; Trucks, G. W.; Schlegel, H. B.; Scuseria, G. E.; Robb, M. A.; Cheeseman, J. R.; Zakrzewski, V. G.; Montgomery, J. A., Jr.; Stratmann, R. E.; Burant, J. C.; Dapprich, S.; Millam, J. M.; Daniels, A. D.; Kudin, K. N.; Strain, M. C.; Farkas, O.; Tomasi, J.; Barone, V.; Cossi, M.; Cammi, R.; Mennucci, B.; Pomelli, C.; Adamo, C.; Clifford, S.; Ochterski, J.; Petersson, G. A.; Ayala, P. Y.; Cui, Q.; Morokuma, K.; Malick, D. K.; Rabuck, A. D.; Raghavachari, K.; Foresman, J. B.; Cioslowski, J.; Ortiz, J. V.; Stefanov, B. B.; Liu, G.; Liashenko, A.; Piskorz, P.; Komaromi, I.; Gomperts, R.; Martin, R. L.; Fox, D. J.; Keith, T.; Al-Laham, M. A.; Peng, C. Y.; Nanayakkara, A.; Gonzalez, C.; Challacombe, M.; Gill, P. M. W.; Johnson, B. G.; Chen, W.; Wong, M. W.; Andres, J. L.; Head-Gordon, M.; Replogle, E. S.; Pople, J. A. *Gaussian 9*8, revision A.7; Gaussian, Inc.: Frisch, M. J. Pittsburgh, PA, 1998.
(31) Lundell, J. *J. Phys. Chem.* **1995**, *99*, 14290.
(32) Lundell, J.; Rasanen; M. *J. Phys. Chem.* **1995**, *99*, 14301.
(33) Lundell, J.; Latajka, Z. *J. Phys. Chem. A* **1997**, *101*, 5004.
(34) Abe, H.; Yamada, K. M. T. *J. Chem. Phys.* **2001**, *114*, 6134.
(35) Oudejans, L.; Miller, R. E. *Chem. Phys. Lett.* **1999**, *306*, 214.
(36) Jessop, P. G.; Ikariya, T.; Noyori, R. *Chem. Rev.* **1995**, *95*, 259.
(37) Duncan, B. N.; Bey, I.; Chin, M.; Mickley, L. J.; Fairlie, T. D.; Martin, R. V.; Matsueda, H. *J. Geophys. Res-Atmos* **2003**, *108*, 4458.
(38) VanDop, H.; Krol, M. *J. Atmos. Chem.* **1996**, *25*, 271.
(39) Piantadosi, C. A.; Zhang, J.; Levin, E. D.; Felz, R. J.; Schmechel, D. E. *Exp. Neurol.* **1997**, *147*, 103.
(40) Piantadosi, C. A.; Zhang, J.; Demchenko, I. T. *Free Radical Bio. Med.* **1997**, *22*, 725.
(41) Hara, S.; Mukai, T.; Kurosaki, K.; Kuriiwa, F.; Watanabe, T.; Kano, S.; Endo, T. *J. Pharmacol. Sci.* **2003**, *91*, Suppl. 1
(42) Yoo, C. S.; Iota, V.; Cynn, H. *Phys. Rev. Lett.* **2001**, *86*, 444.